Nonlinear Rolling of a Biased Ship in a Regular Beam Wave under External and Parametric Excitations

Atef F. El-Bassiouny

Faculty of Science, Mathematics Department, Benha University, Benha 13518, Egypt

Reprint requests to A. F. E.-B.; E-mail: elbassiouny-af@yahoo.com

Z. Naturforsch. **62a**, 573 – 586 (2007); received July 20, 2006

We consider a nonlinear oscillator simultaneously excited by external and parametric functions. The oscillator has a bias parameter that breaks the symmetry of the motion. The example that we use to illustrate the problem is the rolling oscillation of a biased ship in longitudinal waves, but many mechanical systems display similar features. The analysis took into consideration linear, quadratic, cubic, quintic, and seven terms in the polynomial expansion of the relative roll angle. The damping moment consists of the linear term associated with radiation and viscous damping and a cubic term due to frictional resistance and eddies behind bilge keels and hard bilge corners. Two methods (the averaging and the multiple time scales) are used to investigate the first-order approximate analytical solution. The modulation equations of the amplitudes and phases are obtained. These equations are used to obtain the stationary state. The stability of the proposed solution is determined applying Liapunov's first method. Effects of different parameters on the system behaviour are investigated numerically. Results are presented graphically and discussed. The results obtained by two methods are in excellent agreement.

Key words: Nonlinear Rolling; External and Parametric Excitations; Stationary State; Stability.

1. Introduction

The governing equation of a single-degree-of-freedom oscillator typically shows excitations that appear as either an inhohogeneous or a time-varying coefficient in the differential equation. These types of excitations are usually called external and parametric excitations, respectively.

The nonlinearity brings a whole range of phenomena that are not found in linear analysis. These include multiple solutions, jumps, frequency entrapment, natural frequency shift, sub-harmonic, and ultrasubharmonic resonance, period multiplying bifurcation and dynamic chaos [1-7]. It should be noticed that not all these resonance phenomena produced due to the nonlinearity do often occur and are significant in ship motion. Some of them are probably uncommon and may be possibly insignificant. However, the practising naval architect must be able to recognize all such phenomena when they do occur and should understand their consequences so that he will be able to avoid a design that promotes capsizing, to evaluate the sea worthiness of a craft and to recommend appropriate actions to control or minimize the large amplitudes of motions.

The work of Grim [8] and Kerwin [9] showed that the periodic encounter of a ship with a wave results in a time-varying restoring moment, and the roll motion is described by a Mathieu equation. The resonance of these equations reveals the unstable regions and the dangerous frequencies of encounter obtained for small angles, where the linear approximations are valid. Wright and Marshfield [10] performed an interesting analytical and experimental study of nonlinear ship-roll motions. Blocki [11] added a nonlinear damping and nonlinear restoring moment to the roll equation and used it to investigate the probability of capsizing. Cardo et al. [12] used the method of averaging to obtain approximate solutions of the roll equation. They concluded that the roll oscillations are sensitive to the form of the damping model. Mathisen and Price [13] considered damping models in which the nonlinear part is weak in comparison to the linear one. They carried out straightforward perturbation analyses to study free and forced oscillations and showed that their analytical results agree with some experimental data. Nayfeh and Khdeir [14] used a second-order perturbation analysis and presented analytical and numerical results to illustrate different types of nonlinear motions. They also [15] demon-

0932–0784 / 07 / 1000–0573 \$ 06.00 \odot 2007 Verlag der Zeitschrift für Naturforschung, Tübingen \cdot http://znaturforsch.com

strated the occurrence of period multiplying bifurcation and chaos in the nonlinear rolling response of unbiased ships to regular beam waves and [16] investigated the nonlinear rolling of biased ships in regular beam waves. Bass and Haddara [17] examined different roll-damping models used in the literature and presented a scheme to determine the damping coefficients from free-decay data. Schmidt and Tondl [18] investigated the nonlinear rolling motions of ships in longitudinal waves. Falzarano et al. [19] modelled the roll motion by a second-order differential equation with linear and quadratic damping terms and linear and cubic restoring terms. Using closed-form expressions of the heteroclinic and homoclinic manifolds of the unforced and undamped system, they were able to compute the corresponding Melnikov function in closed form, and consequently, to obtain closed-form expressions for the critical values of the forcing at which the homoclinic or heteroclinic bifurcations occur. Nayfeh and Sanchez [20] succeeded in predicting the stability and the complicated nonlinear rolling motion of a ship in beam seas. Bikdash et al. [21] investigated the influence of a general roll-damping on the stability of ships using the Melnikov criterion and characterized the effect of different damping models. Nayfeh and Sanchez [22] studied the chaos and dynamic instability in the rolling motion of ships. El-Bassiouny [23] investigated the principal parametric resonance of a nonlinear mechanical system with two frequencies and self-excitations. Nayfeh et al. [24,25] used a model equation that couples the pitch mode to the roll mode by including the dependence of the pitching moment on the roll orientation. Thus, the pitch (heave) motion is not prescribed but is coupled to the roll motion, and consequently the pitch (heave) and roll orientations are determined simultaneously as functions of a prescribed excitation. They determined first-order uniform expansions that clearly show the significance of the frequency ratio as well as a "saturation" phenomenon which is completely obscured when the pitch or heave motion is specified. Moreover, they offered an explanation of the observations of Froude. Nayfeh [26] considered the nonlinearly coupled roll and pitch motions of a ship in regular head waves in which the couplings are primarily in hydrostatic terms when the pitch frequency is approximately twice the roll frequency and the encounter frequency is near either the pitch or roll natural frequency. He demonstrated the saturation phenomenon when the encounter frequency is near the pitch natural frequency and demonstrated the existence

of Hopf bifurcations. Nayfeh and Sanchez [22, 27] conducted a local-global study with the aid of digital and analog computers and provided results in the form of response curves, bifurcation sets, and basins of safe and capsize regions. They addressed the different routes through which capsizing is likely to occur in regular beam seas. El-Bassiouny [28] studied an approach for implementing an active nonlinear vibration absorber. The strategy exploits the saturation phenomenon that is exhibited by multi-degree-of-freedom systems with cubic nonlinearities possessing one-to-one internal resonance. The proposed technique consists of introducing a second-order controller and coupling it to the plant through a sensor and an actuator, where both the feedback and control signals are cubic.

In this paper, we investigate fundamental resonance and principal parametric resonance of the order one-half for a single-degree-of-freedom system with nonlinearities up to seven terms under external and parametric functions. Two approximate methods are used to find two first-order ordinary differential equations describing the modulation of the amplitudes and phases. Periodic solutions and their stability are determined. Numerical calculations are carried out. The results obtained by the two methods are in excellent agreement.

2. Governing Equation

As shown in Fig. 1, the rolling motion of a biased ship can be described by the absolute roll angle $\phi(t)$ and the relative angle $\theta(t)$ with respect to the local wave slope $\alpha(t)$. Applying Newton's second law, we find that the equation of motion can be written as

$$(I + \delta I)\ddot{\theta} + D(\dot{\vartheta}) + K(\theta, \tau, \gamma) = B - I\ddot{\alpha},$$

$$\theta = \phi - \alpha.$$
(1)

where I is the roll moment of inertia, δI is the added moment of inertia due to the fluid, which is assumed to be constant [5], and B is a constant bias moment, which might be due to steady wind, or a shift in cargo, or water or ice on deck. The righting arm (restoring moment) $K(\theta,\tau,\gamma)$ depends on the angle in which the wave hits the ship and the relative velocity of the wave with respect to the ship. We follow Blocki [11] and obtain the following relation for the rolling of a ship due to heave-roll coupling:

$$K(\theta, \tau, \gamma) = \omega^{2}(\theta + \alpha_{3}\theta^{3} + \alpha_{5}\theta^{5} + \alpha_{7}\theta^{7} + h\cos(\bar{\Omega} + \gamma)),$$
(2)

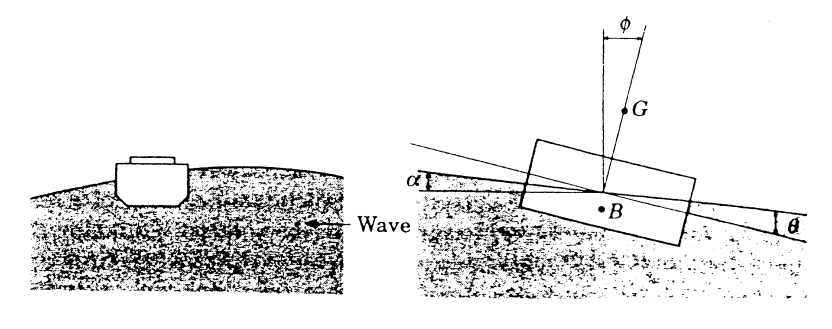


Fig. 1. A ship rolling in longitudinal waves with local wave slope α . The ship is biased at an angle ϕ , so that the relative angle with respect to the wave is $\theta = \phi - \alpha$.

where τ is the time and

$$h = \frac{K_0 a_z}{2\omega_0^2} \tag{3}$$

represents the magnitude of the parametric excitation, which depends on the coupling coefficient $K_{\theta z}$ and the amplitude of the heaving motion a_z . A simple single-degree-of-freedom system is used to describe the basic features of the motion [11]. If we consider the case of waves approaching the ship from the side at an angle γ , the single-degree-of-freedom resulting motion can be described by

$$\begin{split} \ddot{\theta} + 2\mu_{1}\dot{\theta} + \mu_{3}\dot{\theta}^{3} \\ + \omega_{0}^{2}(\theta + \alpha_{3}\theta^{3} + \alpha_{5}\theta^{5} + \alpha_{7}\theta^{7} + h\cos(\bar{\Omega} + \gamma)) \\ = \omega_{0}^{2}(\theta_{s} + \alpha_{3}\theta_{s}^{3} + \alpha_{5}\theta_{s}^{5} + \alpha_{7}\theta_{s}^{7}) \\ + \frac{\alpha_{m}I}{I + \delta I}(\bar{\Omega})^{2}\cos(\bar{\Omega} + \gamma). \end{split} \tag{4}$$

The ship is biased in the sense that it is subjected to a constant heeling that tilts the vessel by an angle θ_s . The wavelength is assumed to be large compared with the ship width. The waves are also assumed to be sinusoidal with a maximum wave slope α_m . The parameter h represents the amplitude of the parametric excitation. It depends on the magnitude of the coupling coefficient and the amplitude of the heaving motion [11, 12]. Equation (4) can be simplified by scaling time according to $t = \omega_0 \tau$, resulting in

$$\ddot{\theta} + \theta + 2\mu_1\dot{\theta} + \mu_3\dot{\theta}^3 + \alpha_3\theta^3 + \alpha_5\theta^5 + \alpha_7\theta^7 + h\theta\cos(\Omega t)$$

$$= \theta_s + \alpha_3\theta_s^3 + \alpha_5\theta_s^5 + \alpha_7\theta_s^7 + F\cos\Omega t,$$
(5)

where

$$F = \frac{\alpha_{\rm m} I \Omega^2}{I + \delta I},\tag{6}$$

and represents the external excitation characterized by the maximum wave slope $\alpha_{\rm m}$. $\theta_{\rm s}$ is the bias angle, Ω the wave frequency, I the ship's interia and δI the fluid's added inertia. The inertia factor is computed with the relation $I = mK^2$. Using the transformation equation $\theta = \theta_{\rm s} + u$, we write (3) as

$$\ddot{u} + u + \varepsilon \left[2\mu_1 \dot{u} + \mu_3 \dot{u}^3 + b_1 u + b_2 u^2 + b_3 u^3 + b_4 u^4 + b_5 u^5 + b_6 u^6 + b_7 u^7 \right] = \varepsilon f \cos \Omega t,$$
(7)

where ε is a small perturbation parameter and

$$b_{1} = 3\alpha_{3}\theta_{s}^{2} + 5\alpha_{5}\theta_{s}^{3} + 3\alpha_{7}\theta_{s}^{6},$$

$$b_{2} = 3\alpha_{3}\theta_{s} + 10\alpha_{5}\theta_{s}^{3} + 21\alpha_{7}\theta_{s}^{5},$$

$$b_{3} = \alpha_{3} + 10\alpha_{5}\theta_{s}^{2} + 35\alpha_{7}\theta_{s}^{4},$$

$$b_{4} = 3\alpha_{5}\theta_{s} + 35\alpha_{7}\theta_{s}^{3},$$

$$b_{5} = \alpha_{5} + 21\alpha_{7}\theta_{s}^{2}, \quad b_{6} = 7\alpha_{7}\theta_{s},$$

$$b_{7} = \alpha_{7}, \quad f = F - h\theta_{s}.$$
(8)

Equation (7) is general and can model a wide variety of oscillators. Our interest is to study the effect of external and parametric functions on systems that can be symmetric or biased.

3. The Averaging Method

The method of averaging is based on the assumption that small perturbations, such as weak nonlinearities or light damping, cause slow (low-frequency) variations in the response of a system [29–31]. The fast (high-frequency) variations due to the perturbations are assumed to be insignificant. Essentially, the averaging approximation yields a simplified mathematical representation of the dynamics of the system by smoothing away these fast variations. Thus, it is of basic importance that the components, which make up the response, be correctly classified as either fast or slow. Usually, the response of each mode is assumed to be of

the form $u_i = a_i \cos(\omega_1 + \beta_i(t))$, where $a_i(t)$ and $\beta_i(t)$ are assumed to be slowly varying. The equations of motion are then transformed into a system of first-order equations for the $a_i(t)$ and $\beta_i(t)$ and, after some manipulation, the equations are integrated with respect to time from 0 to $2\pi/\omega_i$. The averaging approximation consists of the treatment of the slow-varying quantities as constants because they change very little over the period of integration. It is implicitly assumed that the ω_i are not small so that the period $2\pi/\omega_i$ is not large. Thus, we see that the approach where the frequency ω_1 is small cannot be applied.

A alternative strategy for the low-frequency modes can be developed as follows. When $\varepsilon = 0$, the solution of (7) can be written as

$$u = a\cos(t + \varphi),\tag{9}$$

where a and φ are constants. It follows from (9) that

$$\dot{u} = -a\sin(t + \varphi). \tag{10}$$

When $\varepsilon \neq 0$, we assume that the solution of (7) is still given by (9), but with time-varying a and φ . Differentiating (9) with respect to time and recalling that a and φ are functions of t, we have

$$\dot{u} = -a\sin\psi + \dot{a}\cos\psi - a\dot{\varphi}\sin\psi, \tag{11}$$

where

$$\psi = t + \varphi. \tag{12}$$

Comparing (10) with (11), we obtain

$$\dot{a}\cos\psi - a\dot{\varphi}\sin\psi = 0. \tag{13}$$

Differentiating (11) with respect to t, we get

$$\ddot{u} = -a\cos\psi - \dot{a}\sin\psi - a\dot{\phi}\cos\psi. \tag{14}$$

Inserting (9), (10) and (14) into (7), we obtain

$$\dot{a}\sin\psi + a\dot{\varphi}\cos\psi = \\ \varepsilon \left[-2\mu_{1}a\sin\psi - \mu_{3}a^{3}\sin^{3}\psi + b_{1}a\cos\psi \right. \\ \left. + b_{2}a^{2}\cos^{2}\psi + b_{3}a^{3}\cos^{3}\psi + b_{4}a^{4}\cos^{4}\psi \right. (15) \\ \left. + b_{5}a^{5}\cos^{5}\psi + b_{6}a^{6}\cos^{6}\psi + b_{7}a^{7}\cos^{7}\psi \right. \\ \left. + ha\cos\Omega t - f\cos\Omega t \right].$$

Solving (13) and (15) using \dot{a} and $\dot{\phi}$ and using the trigonometric identities gives the following variational equations:

$$\dot{a} = \varepsilon \bigg[-2\mu_1 a (1 - \cos 2\psi) \bigg]$$

A. F. El-Bassiouny · Nonlinear Rolling of a Biased Ship $+\mu_3 a^3 \left(\frac{3}{8} - \frac{1}{2}\cos 2\psi + \frac{1}{8}\cos 4\psi\right) + \frac{1}{2}b_1 a\sin 2\psi$ $+b_2a^2\left(\frac{1}{4}\sin 3\psi - \frac{1}{2}\sin \psi\right)$ $+b_3a^3\left(\frac{1}{16}\sin 2\psi + \frac{1}{8}\sin 4\psi\right)$ $+b_4a^4\left(\frac{1}{8}\sin\psi+\frac{3}{16}\sin3\psi+\frac{1}{16}\sin5\psi\right)$ $+b_5a^5\left(\frac{5}{22}\sin 2\psi + \frac{3}{22}\sin 4\psi + \frac{1}{16}\sin 6\psi\right)$ $+b_6a^6\left(\frac{5}{64}\sin\psi+\frac{9}{64}\sin3\psi+\frac{1}{16}\sin5\psi+\frac{1}{32}\sin7\psi\right)$ $+b_7a^7\left(\frac{1}{8}\sin 2\psi + \frac{5}{256}\sin 4\psi + \frac{7}{256}\sin 6\psi\right)$ $+\frac{1}{64}\sin 8\psi$ $+\frac{1}{4}ha(\sin(\Omega t+2\psi)-\sin(\Omega t-2\psi))$ $-\frac{1}{2}f(\sin(\Omega t + \psi) - \sin(\Omega t - \psi))$, (16) $\dot{\varphi} = \varepsilon \left| -\mu_1 \sin 2\psi \right|$ $-\mu_3 a^2 \left(\frac{1}{16}\sin 2\psi - \frac{1}{8}\sin 4\psi\right) + \frac{1}{2}b_1(1+\cos 2\psi)$ $+b_2a\left(\frac{3}{9}\cos\psi+\frac{1}{4}\cos3\psi\right)$ $+b_3a^2\left(\frac{3}{8}+\frac{1}{2}\cos 2\psi+\frac{1}{8}\cos 4\psi\right)$ $+b_4a^3\left(\frac{5}{8}\cos\psi+\frac{5}{16}\cos3\psi+\frac{1}{16}\cos5\psi\right)$ $+b_5a^4\left(\frac{5}{16}+\frac{5}{22}\cos 2\psi+\frac{3}{16}\cos 4\psi+\frac{1}{22}\cos 6\psi\right)$ $+b_6a^5\left(\frac{43}{64}\cos\psi+\frac{27}{128}\cos3\psi+\frac{11}{128}\cos5\psi\right)$ $+\frac{1}{64}\cos 7\psi$ $+b_7a^6\left(\frac{35}{128}+\frac{15}{32}\cos 2\psi+\frac{7}{32}\cos 4\psi\right)$ $+\frac{1}{16}\cos 6\psi + \frac{11}{128}\cos 8\psi$ $+\frac{1}{2}h\left(\cos\Omega t+\frac{1}{2}\cos(\Omega t+2\psi)-\frac{1}{2}\cos(\Omega t-2\psi)\right)$ $-\frac{f}{2a}(\cos(\Omega t + \psi) - \cos(\Omega t - \psi)) \bigg|.$ (17) The study is focused on two cases of resonance (fundamental resonance and principal parametric resonance). Then from (16) and (17) we take only the constant terms and the terms of small frequency, thus we have

$$\bar{F}_1(y,t) = \bar{f}(y,t) = \begin{bmatrix} \bar{f}_{1a}(y,t) \\ \bar{f}_{1\varphi}(y,t) \end{bmatrix}, \quad y = \begin{bmatrix} A \\ \Phi \end{bmatrix},$$
 (18)

where

$$\bar{f}_{1a}(y,t) = \varepsilon \left[-2\mu_1 A - \frac{3}{8}\mu_3 A^3 + \frac{1}{2}f\sin[(\Omega - 1)t - \Phi] \right]$$

$$-\frac{1}{4}hA\sin[(\Omega - 2)t - 2\Phi] , \qquad (19)$$

$$\bar{f}_{1\varphi}(y,t) = \varepsilon \left[\frac{1}{2}b_1 + \frac{3}{8}b_3 A^2 + \frac{5}{16}b_5 A^4 + \frac{35}{128}b_7 A^6 \right]$$

$$-\frac{f}{2A}\cos[(\Omega - 1)t - \Phi]$$

$$+\frac{1}{4}h\cos[(\Omega - 2)t - 2\Phi] , \qquad (20)$$

and the terms of higher frequency are

$$\bar{f}_1(y,t) = \bar{f}(y,t) = \begin{bmatrix} \bar{f}_{1a}(y,t) \\ \bar{f}_{1\varphi}(y,t) \end{bmatrix}, \tag{21}$$

where

$$\bar{f}_{1a}(y,t) = -2\mu_1 A \cos 2\psi
-\mu_3 A^3 \left(\frac{1}{2}\cos 2\psi + \frac{1}{8}\cos 4\psi\right) + \frac{1}{2}b_1 a \sin 2\psi
+b_2 A^2 \left(\frac{1}{4}\sin 3\psi - \frac{1}{8}\sin \psi\right)
+b_3 A^3 \left(\frac{1}{16}\sin 2\psi + \frac{1}{8}\sin 4\psi\right)
+b_4 A^4 \left(\frac{1}{8}\sin \psi + \frac{3}{16}\sin 3\psi + \frac{1}{16}\sin 6\psi\right)
+b_5 A^5 \left(\frac{5}{32}\sin 2\psi + \frac{3}{32}\sin 4\psi + \frac{1}{16}\sin 6\psi\right)
+b_6 A^6 \left(\frac{5}{64}\sin \psi + \frac{9}{64}\sin 3\psi + \frac{1}{16}\sin 5\psi + \frac{1}{32}\sin 7\psi\right)
+b_7 A^7 \left(\frac{1}{8}\sin 2\psi + \frac{5}{256}\sin 4\psi + \frac{7}{256}\sin 6\psi
+\frac{1}{64}\sin 8\psi\right) + \frac{1}{4}hA\sin(\Omega t + 2\psi)
-\frac{1}{2}f\sin(\Omega t + \psi), \tag{22}$$

$$\bar{f}_{1\varphi}(y,t) = -\mu_1 \sin 2\psi - \mu_3 A^2 \left(\frac{1}{16}\cos 2\psi + \frac{1}{8}\cos 4\psi\right)
+ \frac{1}{2}b_1 \cos 2\psi + b_2 A \left(\frac{3}{8}\cos \psi + \frac{1}{4}\cos 3\psi\right)
+ b_3 A^2 \left(\frac{1}{2}\cos 2\psi + \frac{1}{8}\cos 4\psi\right)
+ b_4 A^3 \left(\frac{5}{8}\cos \psi + \frac{5}{16}\cos 3\psi + \frac{1}{16}\cos 5\psi\right)
+ b_5 A^4 \left(\frac{5}{32}\cos 2\psi + \frac{3}{16}\cos 4\psi + \frac{1}{32}\cos 6\psi\right)
+ b_6 A^5 \left(\frac{43}{64}\cos \psi + \frac{27}{128}\cos 3\psi + \frac{11}{128}\cos 5\psi\right)
+ \frac{1}{64}\cos 7\psi\right) + b_7 A^6 \left(\frac{15}{32}\cos 2\psi + \frac{7}{32}\cos 4\psi\right)
+ \frac{1}{16}\cos 6\psi + \frac{1}{64}\cos 8\psi\right)
+ \frac{1}{4}h\cos(\Omega t + 2\psi) - \frac{f}{2A}\cos(\Omega t + \psi). \tag{23}$$

Then the reduced system to the first approximation takes the form

$$\begin{bmatrix} \dot{A} \\ \dot{\Phi} \end{bmatrix} = \varepsilon \bar{F}_1(y, t), \tag{24}$$

i.e.,

$$\dot{A} = \varepsilon \left[-2\mu_1 A - \frac{3}{8}\mu_3 A^3 + \frac{1}{2}f\sin[(\Omega - 1)t - \Phi] \right]$$

$$-\frac{1}{4}hA\sin[(\Omega - 2)t - 2\Phi] , \qquad (25)$$

$$\dot{\Phi} = \varepsilon \left[\frac{1}{2}b_1 + \frac{3}{8}b_3 A^2 + \frac{5}{16}b_5 A^4 + \frac{35}{128}b_7 A^6 \right]$$

$$-\frac{f}{2A}\cos[(\Omega - 1)t - \Phi] + \frac{1}{4}h\cos[\Omega - 2)t - 2\Phi] . \qquad (26)$$

Since t appear explicitly in (25) and (26), they are called a nonautonomous system. It is convenient to eliminate the explicit dependence on t, thereby transforming the equations into an autonomous system. This can be accomplished by introducing the new dependent variables γ_1 and γ_2 defined by

$$\gamma_1 = (\Omega - 1)t - \Phi = \varepsilon \sigma_1 t - \Phi,
\gamma_2 = (\Omega - 2)t - 2\Phi = \varepsilon \sigma_2 t - 2\Phi,$$
(27)

where σ_1 and σ_2 are the detuning parameters. Inserting (27) into (25) and (26), one obtains the autonomous system that describes the modulations of the amplitude and phase:

$$\dot{A} = \varepsilon \left[-\mu_1 A - \frac{3}{8} \mu_3 A^3 + \frac{1}{2} f \sin \gamma_1 - \frac{1}{4} h A \sin \gamma_2 \right], (28)$$

$$\dot{\Phi} = \varepsilon \left[\frac{1}{2} b_1 + \frac{3}{8} b_3 A^2 + \frac{5}{16} b_5 A^4 + \frac{35}{128} b_7 A^6 - \frac{f}{2A} \cos \gamma_1 + \frac{1}{4} h \cos \gamma_2 \right].$$
 (29)

Two cases of resonance are considered:

3.1. First Case: Fundamental Resonance

In this case, the modulations of the amplitude and phase become

$$\dot{A} = \varepsilon \left[-\mu_1 A - \frac{3}{8} \mu_3 A^3 + \frac{1}{2} f \sin \gamma_1 \right],$$
 (30)

$$\dot{\Phi} = \varepsilon \left[\frac{1}{2} b_1 + \frac{3}{8} b_3 A^2 + \frac{5}{16} b_5 A^4 + \frac{35}{128} b_7 A^6 - \frac{f}{2A} \cos \gamma_1 \right].$$
(31)

We proceed by solving the fixed points of (30) and (31), which correspond to periodic solutions of (7). We set $\dot{a} = \dot{\gamma}_1 = 0$ and obtain

$$-\mu_1 A - \frac{3}{8}\mu_3 A^3 + \frac{1}{2}f\sin\gamma_1 = 0, \tag{32}$$

$$\sigma_{1} - \frac{1}{2}b_{1} - \frac{3}{8}b_{3}A^{2} - \frac{5}{16}b_{5}A^{4} - \frac{35}{128}b_{7}A^{6} + \frac{f}{2A}\cos\gamma_{1} = 0.$$
(33)

Eliminating γ_1 from (31) and (32) yields the frequency response equation

$$\left\{ \left(\mu_1 - \frac{3}{8}\mu_3 A^2 \right)^2 + \left(\sigma_1 - \frac{1}{2}b_1 - \frac{3}{8}b_3 A^2 - \frac{5}{16}b_5 A^4 - \frac{35}{128}b_7 A^6 \right)^2 \right\} A^2 - \frac{1}{4}f^2 = 0.$$
(34)

The stability of the steady-state solutions is considered by Liapunov's first method. Let

$$a = a_0 + a_1$$
, $\gamma_n = \gamma_{n0} + \gamma_{n1}$ $(n = 1, 2)$, (35)

where a_0 and γ_{n0} are the steady-state values and a_1 and γ_{n1} are the infinitesimal time-dependent perturbation. Substituting expressions (35), when n = 1, into (30) and (31) and using steady-state equations, one obtains

$$\dot{A}_1 = \left(-\mu_1 - \frac{9}{8}\mu_3 A_0^2\right) A_1 + \frac{1}{2} (f\cos\gamma_{10})\gamma_{11}, (36)$$

$$\dot{\gamma}_{11} = \left(\frac{\sigma_1}{A_0} - \frac{1}{2A_0}b_1 - \frac{9}{8}b_3A_0 - \frac{25}{16}b_5A_0^3 + \frac{245}{128}b_7A_0^5\right)A_1$$

$$-\frac{1}{2}(f\sin\gamma_{10})\gamma_{11}.$$
(37)

The stability of a given fixed point to a disturbance proportional to $\exp(\lambda t)$ is determined by the roots of

$$\begin{bmatrix} -\mu_{1} - \frac{9}{8}\mu_{3}A_{0}^{2} & \frac{1}{2}f\cos\gamma_{10} \\ \frac{\sigma_{1}}{A_{0}} - \frac{1}{2A_{0}}b_{1} - \frac{9}{8}b_{3}A_{0} \\ -\frac{25}{16}b_{5}A_{0}^{3} + \frac{245}{128}b_{7}A_{0}^{5} \end{bmatrix} = 0. (38)$$

Consequently, a nontrivial solution is stable if and only if the real parts of both eigenvalues of the coefficient matrix (38) are less than zero. Solid/dotted lines denote stable/unstable solution on the response curves, respectively.

3.2. Second Case: Principal Parametric Resonance

In this case, the modulations of the amplitude and phase become

$$\dot{A} = \varepsilon \left[-\mu_1 A - \frac{3}{8} \mu_3 A^3 - \frac{1}{4} h A \sin \gamma_2 \right], \tag{39}$$

$$\dot{\Phi} = \varepsilon \left[\frac{1}{2} b_1 + \frac{3}{8} b_3 A^2 + \frac{5}{16} b_5 A^4 + \frac{35}{128} b_7 A^6 + \frac{1}{4} h \cos \gamma_2 \right]. \tag{40}$$

For stationary solutions, we put $\dot{a} = \dot{\gamma}_2 = 0$; then (39) and (40) become

$$-\mu_1 A - \frac{3}{8}\mu_3 A^3 - \frac{1}{4}hA\sin\gamma_2 = 0, \tag{41}$$

$$\frac{1}{2}\sigma_2 A - \frac{1}{2}b_1 A - \frac{3}{8}b_3 A^3 - \frac{5}{16}b_5 A^5
- \frac{35}{128}b_7 A^7 - \frac{1}{4}hA\cos\gamma_2 = 0.$$
(42)

Equations (41) and (42) show that there are two possibilities: a = 0 or $a \neq 0$. When $a \neq 0$, the frequency response equation becomes

$$\left\{ \left(\mu_1 - \frac{3}{8}\mu_3 A^2 \right)^2 + \left(\frac{1}{2}\sigma_2 - \frac{1}{2}b_1 - \frac{3}{8}b_3 A^2 \right) - \frac{5}{16}b_5 A^4 - \frac{35}{128}b_7 A^6 \right)^2 - \frac{1}{16}h^2 = 0.$$
(43)

The stability of the nontrivial solutions can be determined by using the modulation equations (39) and (40), and using the same method as in the above section, we finally obtain

$$\dot{A}_{1} = \left(-\mu_{1} - \frac{9}{8}\mu_{3}A_{0}^{2}\right)A_{1} + \frac{1}{2}(f\cos\gamma_{10})\gamma_{11}, (44)$$

$$\dot{\gamma}_{21} = \left(\frac{\sigma_{2}}{2A_{0}} - \frac{1}{2A_{0}}b_{1} - \frac{9}{8}b_{3}A_{0}\right)$$

$$-\frac{25}{16}b_{5}A_{0}^{3} + \frac{245}{128}b_{7}A_{0}^{5}A_{1}$$

$$-\frac{1}{2}(f\sin\gamma_{10})\gamma_{11}.$$
(45)

4. The Method of Multiple Scales

To determine an approximate solution of (7), we use the method of multiple scales [6, 29, 30, 32]. First, we seek an approximation to u in the form

$$u(t,\varepsilon) = u_0(T_0, T_1) + \varepsilon u_1(T_0, T_1) + \dots,$$
 (46)

where $T_0 = t$ is a fast-time scale and $T_1 = \varepsilon t$ is a slow-time scale characterizing the time evolution of the amplitude and phase of the response. Second, the derivatives with respect to time are expressed in terms of the new time scales as

$$\frac{d}{dt} = D_0 + \varepsilon D_1 + \dots, \quad \frac{d^2}{dt^2} = D_0^2 + 2\varepsilon D_0 D_1 + \dots, \quad (47)$$

where $D_n = \frac{\partial}{\partial T_n}$. Substituting (46) and (47) into (7) and equating coefficients of similar powers of ε leads to

$$D_0^2 u_0 + u_0 = 0, (48)$$

$$D_0^2 u_1 + u_1 = -2D_0 D_1 u_0 + b_1 u_0 - 2\mu (D_0 u_0)$$

$$-\mu_3 (D_0 u_0)^3 - b_2 u_0^2 - b_3 u_0^3 - b_4 u_0^4 - b_5 u_0^5$$
(49)

$$-b_6 u_0^6 - b_7 u_0^7 - ha \cos \Omega t + f \cos \Omega t.$$

The solution of (48) can be expressed as

$$u_0 = A(T_1) \exp(iT_0) + \bar{A}(T_1) \exp(-iT_0),$$
 (50)

where \bar{A} is the complex conjugate of A, which is an arbitrary complex function of T_1 at this level of approximation. It is determined by imposing the solvability condition at this level of approximation.

Substituting (50) into (49) yields

$$D_0^2 u_1 + u_1 = \left[-2iD_1 A + b_1 A - 2i\mu_1 A - 3i\mu_3 A^2 \bar{A} \right.$$

$$-10b_5 A^3 \bar{A}^2 - 35b_7 A^4 \bar{A}^3 + \frac{1}{2} f \right] \exp(it)$$

$$- \left[b_2 A^2 + 4b_4 A^3 \bar{A} + 15b_6 A^4 \bar{A}^2 \right] \exp(2it)$$

$$+ \left[(i\mu_3 - b_3) A^3 - 5b_5 A^4 \bar{A} - 21b_7 A^5 \bar{A}^2 \right] \exp(3it)$$

$$+ \left[-b_4 A^4 - 6b_6 A^5 \bar{A} \right] \exp(4it)$$

$$- \left[b_5 A^5 - 7b_7 A^6 \bar{A} \right] \exp(5it)$$

$$- b_6 A^6 \exp(6it) - 20b_7 A^7 \exp(7it)$$

$$- 2b_2 A \bar{A} - 6b_4 A^2 \bar{A}^2 - 20b_7 A^3 \bar{A}^3 + cc, \tag{51}$$

where cc stands for the complex conjugate of the preceding terms. To describe quantitatively the nearness of Ω to 1 and Ω to 2, we introduce two detuning parameters, σ_1 and σ_2 , defined by

$$\Omega = 1 + \varepsilon \sigma_1, \quad \Omega = 2 + \varepsilon \sigma_2.$$
 (52)

Then, substituting (52) into (51), we find that the secular terms are eliminated from u_1 if

$$2i(D_1A + \mu_1A) - b_1A + 3i\mu_3A^2\bar{A} + 3b_3A^2\bar{A}$$

$$+ 10b_5A^3\bar{A}^2 + 35b_7A^4\bar{A}^3 - \frac{1}{2}\bar{A}h\exp(i\sigma_2T_1) \quad (53)$$

$$-\frac{1}{2}f\exp(i\sigma_1T_1) = 0.$$

Next, we express (53) in real variable by letting

$$A = \frac{1}{2}a(T_1)\exp(i\beta(T_1)).$$
 (54)

Substituting (54) into (53) and separating the real and imaginary parts yields

$$a' = -\mu a - \frac{3}{8}\mu a^2 + \frac{1}{2}f\sin\Gamma_1 - \frac{1}{4}ha\sin\Gamma_2, (55)$$

$$a\beta' = \frac{1}{2}b_1a + \frac{3}{8}b_3a^3 + \frac{5}{16}b_5a^5 + \frac{35}{128}b_7a^7 - \frac{1}{2}f\cos\Gamma_1 + \frac{1}{4}ha\cos\Gamma_2,$$
(56)

where

$$\Gamma_1 = \sigma_1 T_1 - \beta, \quad \Gamma_2 = \sigma_2 T_1 - 2\beta. \tag{57}$$

Stationary solutions of (55) and (56) correspond to $\dot{a} = 0$ and $\dot{\Gamma}_n = 0$ (n = 1, 2). Then it follows from (57) that

$$\beta' = \sigma_1 = \frac{1}{2}\sigma_2 = \sigma,\tag{58}$$

and hence if follows from (55) and (56) that stationary solutions are given by

$$-\mu a - \frac{3}{8}\mu a^2 + \frac{1}{2}f\sin\Gamma_1 - \frac{1}{4}ha\sin\Gamma_2 = 0, (59)$$

$$a\sigma - \frac{1}{2}b_1a - \frac{3}{8}b_3a^3 - \frac{5}{16}b_5a^5 - \frac{35}{128}b_7a^7 + \frac{1}{2}f\cos\Gamma_1 - \frac{1}{4}ha\cos\Gamma_2 = 0.$$
(60)

Two cases of resonances are considered as described in the following sections.

4.1. First Case: Fundamental Resonance

In this case, (59) and (60) become

$$-\mu a - \frac{3}{8}\mu a^2 + \frac{1}{2}f\sin\Gamma_1 = 0, (61)$$

$$a\sigma - \frac{1}{2}b_1a - \frac{3}{8}b_3a^3 - \frac{5}{16}b_5a^5 - \frac{35}{128}b_7a^7 + \frac{1}{2}f\cos\Gamma_1 = 0.$$
 (62)

Squaring (61) and (62) and adding the results gives the frequency response equation

$$\left\{ \left(\mu_1 - \frac{3}{8}\mu_3 a^2 \right)^2 + \left(\sigma_1 - \frac{1}{2}b_1 - \frac{3}{8}b_3 a^2 \right) - \frac{5}{16}b_5 a^4 - \frac{35}{128}b_7 a^6 \right)^2 \right\} a^2 - \frac{1}{4}f^2 = 0,$$
(63)

which is in full agreement with equation (34) obtained by the method of averaging.

4.2. Second Case: Principal Parametric Resonance

In this case, (59) and (60) become

$$-\mu a - \frac{3}{8}\mu a^2 - \frac{1}{4}ha\sin\Gamma_2 = 0,$$
 (64)

A. F. El-Bassiouny · Nonlinear Rolling of a Biased Ship

$$a\sigma - \frac{1}{2}b_1a - \frac{3}{8}b_3a^3 - \frac{5}{16}b_5a^5 - \frac{35}{128}b_7a^7 - \frac{1}{4}ha\cos\Gamma_2 = 0.$$
 (65)

From these equations, we obtain the frequency response equation

$$\left\{ \left(\mu_1 - \frac{3}{8}\mu_3 a^2 \right)^2 + \left(\frac{1}{2}\sigma_2 - \frac{1}{2}b_1 - \frac{3}{8}b_3 a^2 \right) - \frac{5}{16}b_5 a^4 - \frac{35}{128}b_7 a^6 \right)^2 - \frac{1}{16}h^2 = 0,$$
(66)

which is in excellent agreement with (43) obtained by the method of averaging.

5. Numerical Results

In this section the numerical solutions of the frequency response equations are studied. Frequency response equations (34) and (43) are nonlinear algebraic equations in the amplitude (A). The equation and stability conditions are solved numerically. Excitation response and frequency response curves are plotted in Figs. 2–21, which present the variation of the amplitude A against the detuning parameters σ_1 and σ_2 .

Figures 2–11 represent the frequency response curves for fundamental resonance. In Fig. 2, the response amplitude bent to the right which gives hardening behaviour has two branches (single-valued curve and semi-oval) such that the single-valued curve has unstable solutions and the semi-oval has stable and

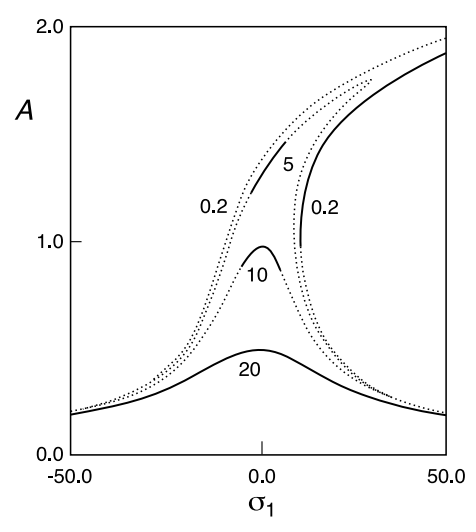


Fig. 2. Variation of the amplitude of the response with the detuning parameter σ_1 for increasing μ_1 .

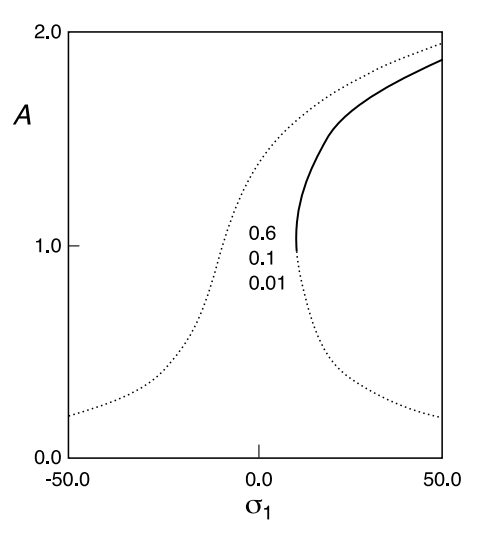


Fig. 3. Variation of the amplitude of the response with the detuning parameter σ_1 for decreasing μ_1 and μ_3 , respectively.

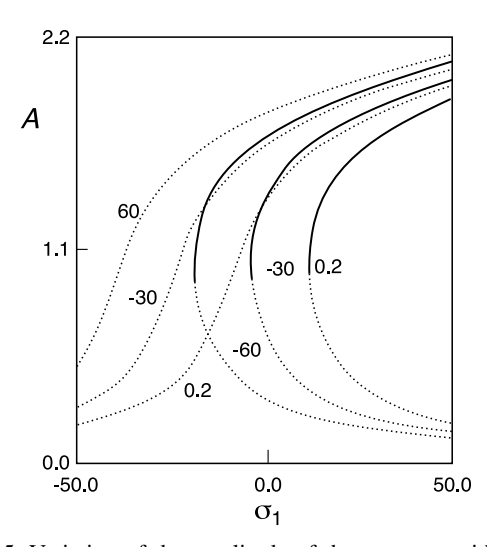


Fig. 5. Variation of the amplitude of the response with the detuning parameter σ_1 for decreasing b_1 .

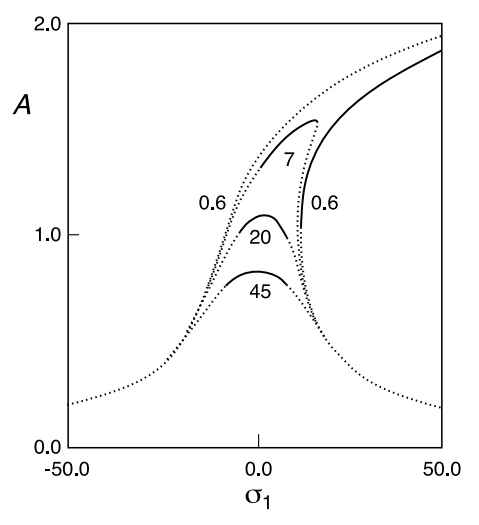


Fig. 4. Variation of the amplitude of the response with the detuning parameter σ_1 for increasing μ_3 .

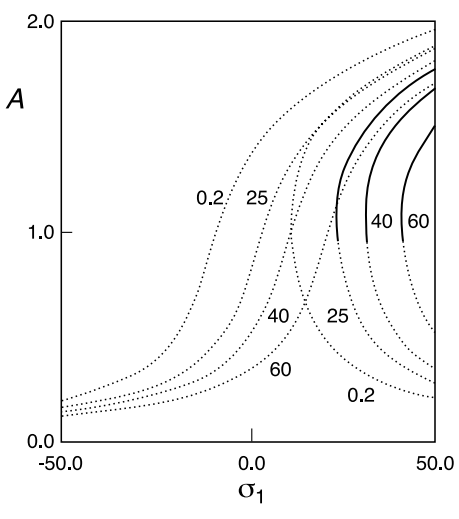


Fig. 6. Variation of the amplitude of the response with the detuning parameter σ_1 for increasing b_1 .

unstable solutions. As σ_1 decreases through the interval [0-50], the response amplitude loses stability via a saddle node bifurcation. As $\mu_1 = 5$ the branches connect and give one continuous curve such that the zone of multi-values and stability is decreased. For further increasing of μ_1 (i. e. μ_1 takes the values 10 and 20), the multi-valued curve disappears and the response amplitude has a decreased single-valued curve; there exist two saddle node bifurcations. When the damping factor μ_1 decreases up to 0.01, we note that the response amplitude is not affected and has the same re-

gion of stability. Also, as the damping factor μ_3 takes the values 0.1 and 0.01, we observe that the response amplitude is not affected and has the same region of stability, Figure 3. For increasing the damping factor μ_3 (i.e. μ_3 takes the values 7, 20 and 45), we get the same variation as in Fig. 1, and the zone of stability is increased; there exist two saddle node bifurcations, Figure 4. When the coefficient of the linear term b_1 is decreased with negative values, we observe that the upper branch has increased magnitudes and a semi-oval shift to the left gives the increase in

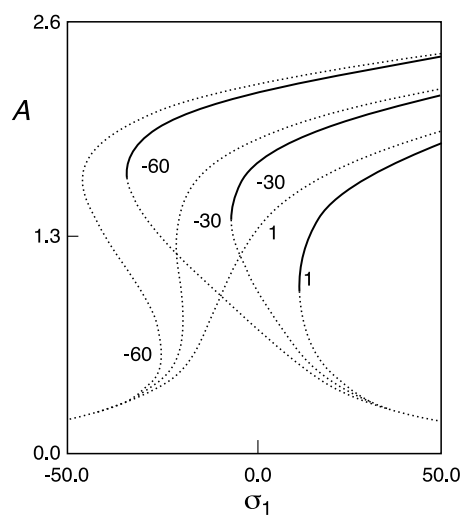


Fig. 7. Variation of the amplitude of the response with the detuning parameter σ_1 for decreasing b_3 .

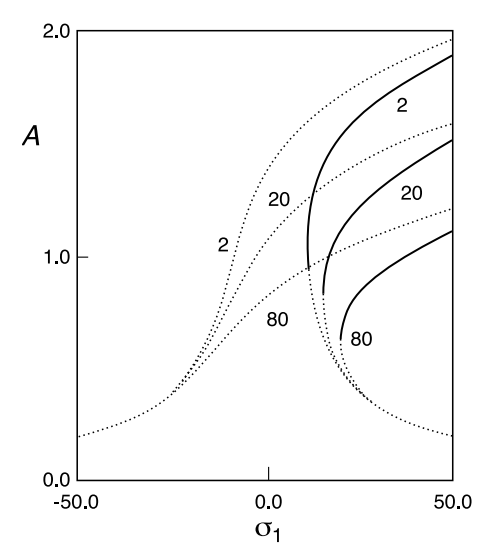


Fig. 8. Variation of the amplitude of the response with the detuning parameter σ_1 for increasing b_5 .

the zones of stability and is multi-valued. The single-valued curve shifts to the top with increased unstable magnitudes and the semi-oval consists of two branches such that the upper branch has increased stable magnitudes and the lower branch has decreased unstable magnitudes, respectively, and there exists one saddle node bifurcation for each semi-oval, Figure 5. As b_1 takes the values 25, 40 and 60, we note that the upper branch moves to the top with increased unstable magnitudes and the semi-oval moves to the right and

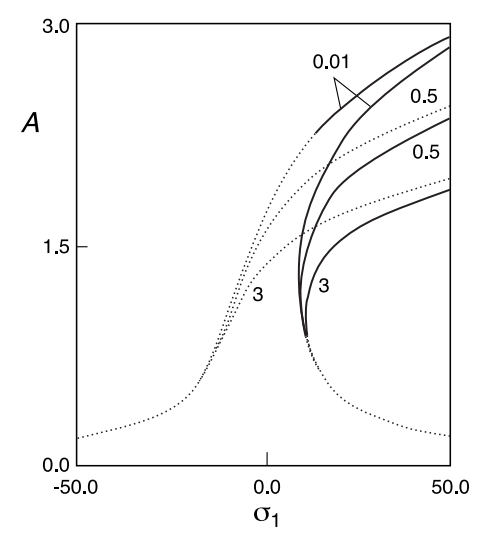


Fig. 9. Variation of the amplitude of the response with the detuning parameter σ_1 for decreasing b_7 .

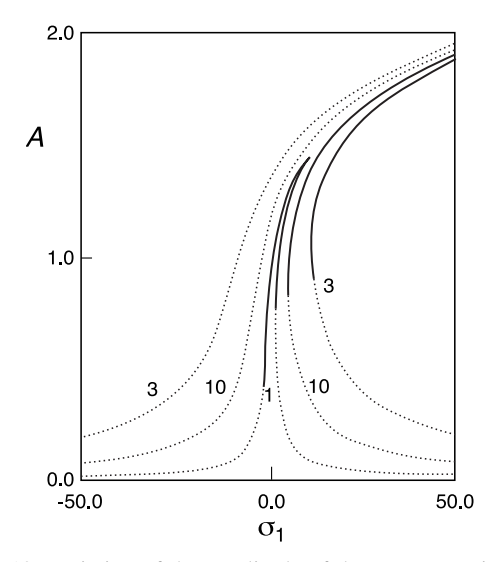


Fig. 10. Variation of the amplitude of the response with the detuning parameter σ_1 for decreasing f.

contracts such that the upper branch has decreased stable magnitudes and the lower branch has increased unstable magnitudes, respectively, and there exists one saddle node bifurcation for each semi-oval, Figure 6. When the coefficient of the cubic nonlinear term b_3 decreases with negative values, we observe that the upper branch has increased magnitudes and a semi-oval shift to the left, respectively, which leads to increasing the regions of stability and multi-valued and there exists one saddle node bifurcation for each semi-

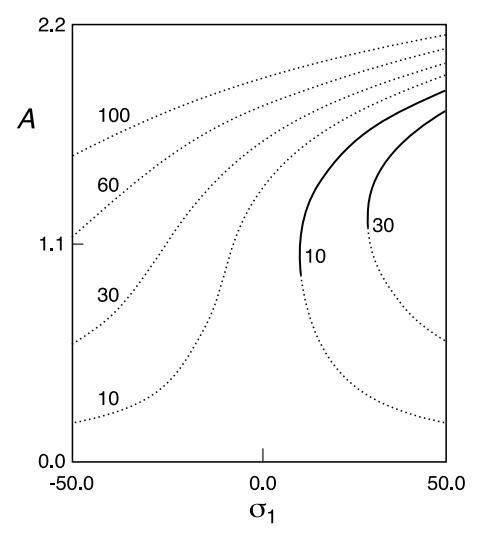


Fig. 11. Variation of the amplitude of the response with the detuning parameter σ_1 for increasing f.

oval, Figure 7. When the coefficient of quintic nonlinear term b_5 takes the values 20 and 80, we observe that the response amplitude has decreased magnitudes. Each semi-oval has one saddle node bifurcation, Figure 8. If the coefficient of the seven nonlinear term b_7 is decreased, we note that the response amplitude has increased magnitudes. The upper branch has stable and unstable solutions and there exist two saddle node bifurcations. Also there exists one saddle node bifurcation for each semi-oval, Figure 9. When the amplitude of external excitation f is decreased, we observe that the upper branch has decreased magnitudes and stable and unstable solutions, and there exist two saddle node bifurcations. Also there exists one saddle node bifurcation in the semi-oval. As σ_1 decreases up to 1, the two branches connect and give a continuous curve such that there exist two saddle node bifurcations, Figure 10. When f is increased up two 30, we observe that the upper branch shifts to the top with unstable increased magnitudes and the semi-oval contracts and decreases in the region of stability and multivalued. As σ_1 decreases through the interval [0-50], the response amplitude loses stability via a saddle node bifurcation. When f takes the values 60 and 100, the semi-oval disappears and the single-valued curve moves to the top with unstable increased magnitudes, Figure 11.

Figures 12-21 represent the frequency response curves for subharmonic resonance of order one-half. In Fig. 12, we observe that the response amplitude has

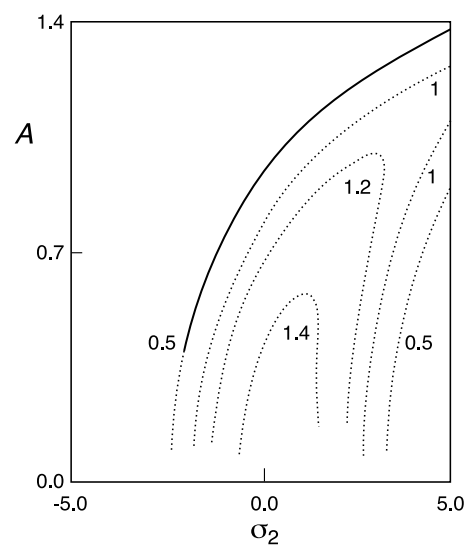


Fig. 12. Variation of the amplitude of the response with the detuning parameter σ_2 for increasing μ_1 .

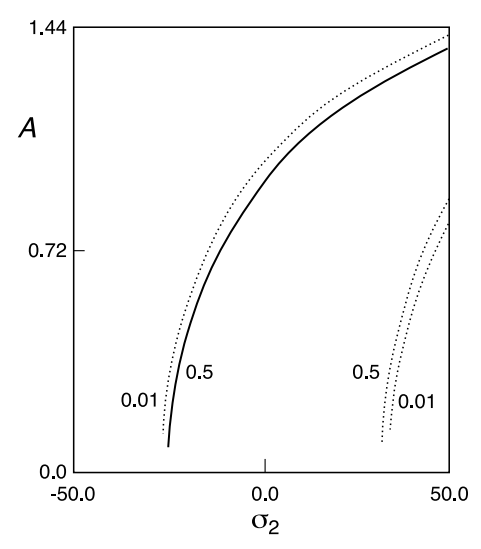


Fig. 13. Variation of the amplitude of the response with the detuning parameter σ_2 for decreasing μ_1 .

two branches which bent to the right and have hardening behaviour. The left branch has stable and unstable solutions, and there exists one saddle node bifurcation, while the right branch has unstable solutions. As the damping factor μ_1 is increased up to 1, the left and right branches shift to the right and left, respectively, such that the left branch has decreased magnitudes and the right branch has increased magnitudes. All solutions are unstable. When $\mu_1 = 1.2$, the two branches contracts and give a semi-closed curve, and all solu-

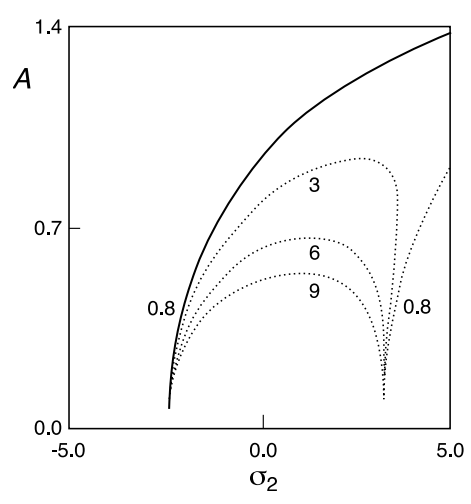


Fig. 14. Variation of the amplitude of the response with the detuning parameter σ_2 for increasing μ_3 .

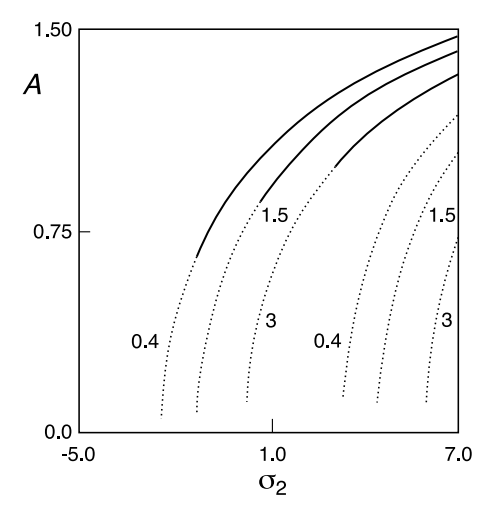


Fig. 15. Variation of the amplitude of the response with the detuning parameter σ_2 for increasing b_1 .

tions are unstable. As $\mu_1 = 1.4$, the semi-closed curve contracts and has unstable decreased magnitudes. The regions of multi-valued and definition are decreased. For decreasing the damping factor μ_1 up to 0.01, we note that the left branch shifts to the left with unstable increased magnitudes and the right branch shifts to the right with unstable decreased magnitudes. The zone of definition is increased, Figure 13. As the damping factor μ_3 takes the values 3, 6 and 9, the two branches contract and give a semi-closed curve which contract, respectively, with unstable decreased magnitudes and defined in the same interval, Figure 14. When the coefficient of the linear term b_1 decreases (i. e. b_1 takes

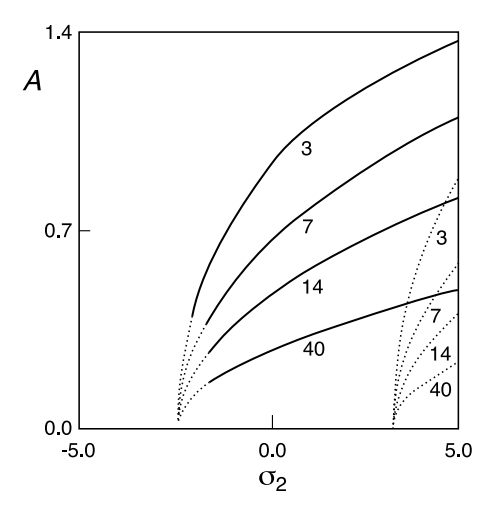


Fig. 16. Variation of the amplitude of the response with the detuning parameter σ_2 for increasing b_3 .

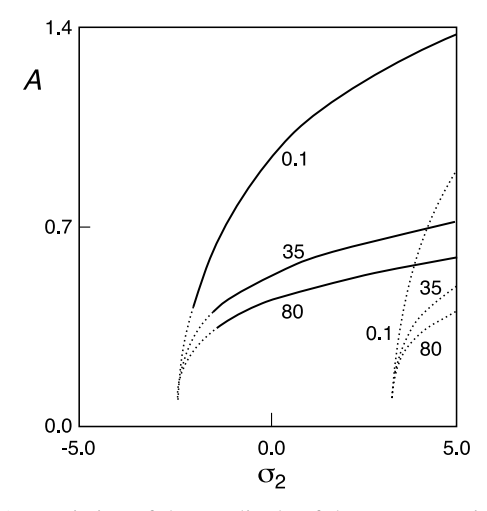


Fig. 17. Variation of the amplitude of the response with the detuning parameter σ_2 for increasing b_5 .

the values 1.5 and 3), we note that the left and right branches are moved to the right with decreased magnitudes. The zones of stability and multi-valued are decreased and there exists one saddle node bifurcation in the left branch, Figure 15. For decreasing the coefficient of the cubic nonlinear term b_3 , we note that the two branches shift down with decreased magnitudes and defined in the same interval. There exists one saddle node bifurcation in the left branch, Figure 16. As the coefficient of the quintic nonlinear term b_5 takes the values 35 and 80, we get the same variation as in Fig. 16, Figure 17. When the coefficient of the seven nonlinear term b_7 increases, we get the same variation

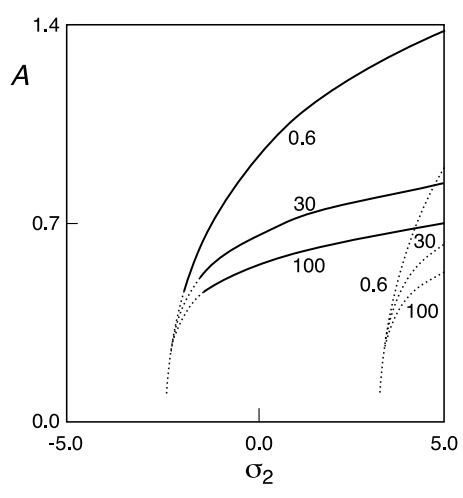


Fig. 18. Variation of the amplitude of the response with the detuning parameter σ_2 for increasing b_7 .

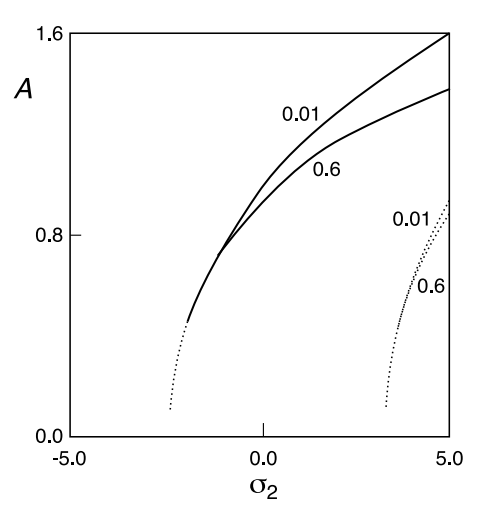


Fig. 19. Variation of the amplitude of the response with the detuning parameter σ_2 for decreasing b_7 .

as in Fig. 16, Figure 18. For decreasing b_7 up to 0.01, we note that the left branch shifts to the top and has increased magnitudes such that the zone of stability decreases and there exist two saddle node bifurcations. The right branch has increased magnitudes in a small interval, Figure 19. As the amplitude of external excitation h takes the values 10 and 15, we observe that the left and right branches shift to the left and right with increased and decreased magnitudes, respectively, and the region of definition and multi-valued are increased and decreased, respectively, Figure 20. For increasing h, we get the same variation as in Fig. 12, Figure 21.

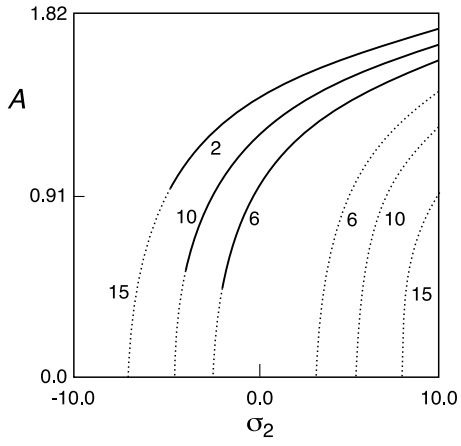


Fig. 20. Variation of the amplitude of the response with the detuning parameter σ_2 for increasing h.

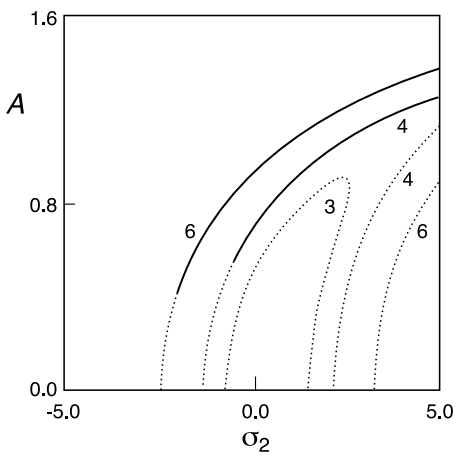


Fig. 21. Variation of the amplitude of the response with the detuning parameter σ_2 for decreasing h.

6. Summary and Conclusion

Two methods (the averaging and the multiple time scales) are used to investigate first-order approximate analytical solutions of the nonlinear rolling response of a ship in regular beam seas. The analysis took into consideration linear, quadratic, cubic, quintic, and seven terms in the polynomial expansion of the relative roll angle. The damping moment consists of the linear term associated with radiation and viscous damping and a cubic term due to frictional resistance and eddies behind bilge keels and hard bilge corners. The modulation equations (reduced equations) of the amplitude and phase are obtained. Steady-state solutions and their stability are determined. The following conclusions can be deduced from the analysis:

From the frequency response curves of primary resonance, we observe that the response amplitude consists of two branches (single-valued curve and semi-oval) which is bending to the right and has hardening behaviour. The response amplitude is not affected and has the same region of stability when μ_1 and μ_3 increase and when f=1. The multi-valued disappears when $\mu_1=10$ and $\mu_3=20$.

From the frequency response curves of subharmonic resonance of order one-half, we note that the response

- [1] A.H. Nayfeh and D.T. Mook, Non-Linear Oscillations, Wiley-Interscience, New York 1979.
- [2] G. Guckenheimer and P. Holmes, Non-Linear Oscillations, Dynamical System, and Bifurcations of Vector Fields, Springer-Verlag, New York 1983.
- [3] A. H. Nayfeh and B. Balachandran, Applied Non-Linear Dynamic, Wiley-Interscience, New York 1994.
- [4] S. Natsiavas and S. Theodossiades, Int. J. Non-Linear Mech. 33, 843 (1998).
- [5] A. R. F. Elhefnawy and A. F. El-Bassiouny, Chaos, Solitons and Fractals 23, 289 (2004).
- [6] A. F. El-Bassiouny, Chaos, Solitons and Fractals, 30, 1098 (2005).
- [7] A. F. El-Bassiouny, Physica A 366, 167 (2006).
- [8] O. Grim, Schiffstechnik 2, 10 (1955).
- [9] J. E. Kerwin, Int. Shipbuild. Prog. 2, 597 (1955).
- [10] J. H. Wright and W. B. Marshfield, Trans. R. Inst. Naval Architects 122, 129 (1979).
- [11] W. Blocki, Int. Shipbuild. Prog. 27, 36 (1980).
- [12] A. Cardo, A. Francescutto, and R. Nabergoj, Ocean Eng. 9, 171 (1982).
- [13] J. B. Mathisen and W. G. Price, Trans. R. Inst. Naval Architects 127, 295 (1984).
- [14] A. H. Nayfeh and A. A. Khdeir, Int. Shipbuild. Prog. 33, 40 (1986).
- [15] A. H. Nayfeh and A. A. Khdeir, Int. Shipbuild. Prog. 33, 379 (1986).
- [16] A. H. Nayfeh and A. A. Khdeir, Int. Shipbuild. Prog. 33, 12 (1986).
- [17] D. W. Bass and M. R. Haddara, Int. Shipbuild. Prog. 35, 5 (1988).

amplitude consists of two branches which are bending to the right and have hardening behaviour. The zone of definition increases when μ_1 is decreasing and h is increasing. The response amplitude loses stability when μ_1 and μ_3 are increasing and μ_1 is decreasing. The two branches contract and give a continuous curve when μ_1 and μ_3 are increasing and h is decreasing. The two branches have the same region of definition when μ_1 , b_1 , b_3 , b_5 , b_7 are increasing and b_7 is decreasing.

- [18] G. Schmidt and A. Tondl, Int. Shipbuild. Prog. 37, 247 (1990).
- [19] J. M. Falzarano, S. W. Shaw, and A. W. Troesh, Int. J. Bifurcation and Chaos 2, 101 (1992).
- [20] N. E. Sanchez and A. H. Nayfeh, Int. Shipbuild. Prog. 33, 411 (1990).
- [21] M. Bikdash, B. Balachandran, and A. H. Nayfeh, Nonlinear Dynamics 6, 101 (1994).
- [22] A. H. Nayfeh and N. E. Sanchez, Chaos and dynamic instability in the rolling motion of ships, Proceedings of the 17th Symposium on Naval Hydrodynamics, The Hague, The Netherlands, August 29 September 3, 1998.
- [23] A. F. El-Bassiouny, Mech. Res. Commun. 32, 337 (2005).
- [24] A. H. Nayfeh, D. T. Mook, and L. R. Marshall, J. Hydronaut. 7, 145 (1973).
- [25] A. H. Nayfeh, D. T. Mook, and L. R. Marshall, J. Hydronaut. 8, 130 (1974).
- [26] A. H. Nayfeh, J. Ship Res. 32, 92 (1988).
- [27] A. H. Nayfeh and N. E. Sanchez, Int. Shipbuild. Prog. 37, 331 (1990).
- [28] A. F. El-Bassiouny, Phys. Scr. 72, 203 (2005).
- [29] A. H. Nayfeh, Perturbation Methods, Wiley-Interscience, New York 1973.
- [30] A. H. Nayfeh, Introduction to Perturbation Techniques, Wiley-Interscience, New York 1981.
- [31] A. M. Elnaggar and A. F. El-Bassiouny, Second ICEMP, Cario, Egypt, 1994, pp. 63–82.
- [32] A. M. Elnaggar and A. F. El-Bassiouny, Acta Mech. Sin. 9, 61 (1993).